Applied Catalysis A: General 447–448 (2012) 1–6

Contents lists available at SciVerse ScienceDirect

Applied Catalysis A: General

journal homepage: www.elsevier.com/locate/apcata

Effect of support on V_2O_5 catalytic activity in chlorobenzene oxidation

Chiraz Gannoun[a,*], Romain Delaigle[b], Damien P. Debecker[b], Pierre Eloy[b], Abdelhamid Ghorbel[a], Eric M. Gaigneaux[b]

[a] Laboratoire de Chimie des Matériaux et Catalyse, Département de Chimie, Faculté des Sciences de Tunis, Campus universitaire, 2092 El Manar Tunis, Tunisia
[b] Université catholique de Louvain, Institute of Condensed Matter and Nanosciences (IMCN), Division «Solids, Molecules and ReactiviTy (MOST)», Croix du Sud 2/17, B-1348 Louvain-la-Neuve, Belgium

ARTICLE INFO

Article history:
Received 21 May 2012
Received in revised form 23 July 2012
Accepted 15 August 2012
Available online 1 September 2012

Keywords:
Aerogel
Sulfate
Cerium
Vanadia–titania
Chlorobenzene oxidation

ABSTRACT

The present paper investigates the influence of the direct incorporation of ceria in TiO_2 aerogels support (sulfated and unsulfated) prepared by a sol–gel route on the catalytic properties of vanadia based materials in the total oxidation of chlorobenzene. ICP-AES, N_2 physisorption, XRD, DRIFTS, Raman spectroscopy, XPS, H_2-TPR and NH_3-TPD were employed for catalyst characterization. This study demonstrated that cerium oxide is present as CeO_2 form at the catalyst surface, which can improve the catalyst redox properties and so enhance the catalytic activity at high temperature (400 °C). Besides, sulfate containing vanadia–titania samples (doped or not with ceria) had their catalytic performances considerably improved (due to sulfates) at lower temperatures (range 200–300 °C). This is due to an increased global acidity and higher reactivity of redox sites thanks to the superficial interaction between (i) vanadia and sulfate, and (ii) when ceria is present, between ceria and sulfate leading to higher efficiency of catalysts in the chlorobenzene oxidation.

1. Introduction

Chlorinated volatile organic compounds (Cl-VOCs) are major contributors to air pollution because of their highly toxic nature [1]. A large number of methods have been applied in order to solve the problem of atmospheric release of chlorinated VOCs (typically adsorption, thermal incineration, hydrodechlorination, biological process, steam reforming, photocatalytic degradation, etc.) [2–7]. However, there is still a need for research on techniques, which are economical, more favorable and truly able to destroy the pollutants rather than merely displace and dispose them. The catalytic destruction of chlorinated VOC to CO_x, H_2O and HCl appears very promising in this context [4,6,8–12].

Supported vanadium oxide constitutes a very important class of catalytic materials resistant against chlorinated volatile organic compounds [10,12–14]. In the literature, studies indicated that the nature of the support plays a crucial role in catalytic properties since the metal oxide-support interaction affects redox, acid–base properties and dispersion of the active phase [15,16]. Titania supports seem to be the most indicated. In addition to their good mechanical, thermal, and anticorrosive properties, they favor the spreading of VO_x active phase in the form well-dispersed monolayer [17]. Furthermore, it has been shown that the addition of SO_4^{2-} species to TiO_2 enhances the acidity and can lead to a better activity in chlorinated VOCs oxidation [10,12,18–21]. The beneficial effect of the sulfated TiO_2 is due to an increase of the amount of Brønsted acid sites which promote the adsorption of the aromatics on the support, and of strong Lewis sites which improve the spreading of VO_x phase on the surface of the catalysts [10,17].

Titania doped with CeO_2 is yet another interesting support since CeO_2 exhibits excellent redox properties due to its prominent ability to shift between Ce^{3+} and Ce^{4+} under oxidizing and reducing conditions respectively. Labile oxygen vacancies form easily and the mobility of bulk oxygen species is high [22,23]. Indeed, the mixing of the two different oxides TiO_2 and CeO_2 could bring new stable compounds that may lead to totally different physicochemical properties and catalytic behavior [24].

CeO_2–TiO_2 mixed oxide was studied in various applications, either as support or as catalyst, such as catalytic wet air oxidation reactions of organic compounds [25], NO removal [26] and Diesel soot combustion [27]. Huang et al. introduced CeO_2 to V_2O_5/TiO_2 formulations and demonstrated that V_2O_5/CeO_2–TiO_2 catalysts exhibit higher activity than V_2O_5–TiO_2 in the selective catalytic reduction (SCR) of NO to N_2 with NH_3 (NO conversion is 99.2% at 165 °C) [28]. Xu et al. successfully developed a CeO_2/TiO_2 catalyst by impregnation method for the NH_3-SCR of NO_x in the temperature range of 275–400 °C [29] (NO conversion greater than 92%). Similarly, Gao et al. proposed a Ceria titania mixed oxide system, prepared by sol gel route, as very efficient catalyst for the SCR process in the temperature range of 300–400 °C (NO_x conversion

* Corresponding author. Tel.: +216 96 940 755; fax: +216 96 940 755.
E-mail address: gannoun.chiraz@gmail.com (C. Gannoun).

0926-860X/$ – see front matter © 2012 Elsevier B.V. All rights reserved.
http://dx.doi.org/10.1016/j.apcata.2012.08.034

exceeds 95%) [30]. Besides, Shan et al. developed CeO_2/TiO_2 catalyst by homogeneous precipitation method for NH_3-SCR of NO_x [31]. The catalyst exhibited good catalytic performance (over 90% NO_x conversion from 250 to 450 °C).

Based on the fact that the good catalysts for SCR are also efficient in the oxidation of chlorinated VOCs and motivated by the favorable characteristics of ceria-based mixed oxides, we thus investigate in this study the direct incorporation of cerium species in the TiO_2 support (sulfated or not sulfated) and hope to achieve a good activity of the supported vanadia in the total oxidation of chlorobenzene.

V_2O_5/TiO_2, $V_2O_5/TiO_2–SO_4^{2-}$, $V_2O_5/TiO_2–CeO_2$ and $V_2O_5/TiO_2–SO_4^{2-}–CeO_2$ catalysts were synthesized by impregnation method. The amount of vanadia oxide is fixed to be small (2 wt.%) due to the requirement in the industrial practice in order to limit the oxidation of SO_2 to SO_3 as much as possible in the case of the elimination of Cl-VOCs from sulfur bearing fuels [32].

The supports (TiO_2, $TiO_2–SO_4^{2-}$, $TiO_2–CeO_2$ and $TiO_2–SO_4^{2-}–CeO_2$) were elaborated by a one step sol–gel method and transformed into aerogels using a supercritical drying process [12]. The structural, textural, acidic and redox properties of the catalysts have been characterized by ICP-AES, XRD, N_2-physisorption, DRIFTS, Raman spectroscopy, NH_3-TPD and H_2-TPR.

2. Experimental

2.1. Catalysts preparation

Four kinds of TiO_2 supports (TiO_2, $TiO_2–SO_4^{2-}$, $TiO_2–CeO_2$ and $TiO_2–SO_4^{2-}–CeO_2$) were prepared via sol–gel method as follows: Titanium (IV) isopropoxide (Aldrich, 98%), as precursor, with anhydrous ethanol (Aldrich, 98%), as solvent, was chemically modified by adding acetylacetone (Fluka, 99%) according to a molar ratio acetylacetone/Ti = 1 in order to control hydrolysis and condensation reaction rates. This solution was maintained for 1 h under stirring. To obtain mixed ceria titania oxide, cerium nitrate (Aldrich, 99.5%) was added to the organic mixture according to a molar ratio Ce/Ti = 0.1. To obtain sulfated supports, sulfuric acid (Fluka, 96%) was added according to a molar ratio S/Ti = 0.2. Homogenous gels are obtained by hydrolysis and condensation after HNO_3 supply. The amount of distilled water added corresponded to the molar ratio H_2O/Ti = 10. The gels were, thereafter, transformed into aerogels by drying under supercritical conditions of ethanol (P = 63 bars, T = 243 °C) and are denoted Ti, TiS, TiCe and TiSCe. Then, corresponding catalysts with theoretical vanadia loading of 2 wt.% were synthesized by impregnating 2 g of support with 4 ml of an acetone solution of vanadyl acetylacetonate (Fluka, 95%). The obtained wet solids are then dried in an oven at 60 °C for 24 h. Finally, catalysts are calcined for 12 h at 500 °C under flowing O_2 (30 ml/min) and denoted respectively VTi, VTiS, VTiCe and VTiSCe.

2.2. Characterization of catalysts

The elemental analysis was performed by inductively coupled plasma-atomic emission spectroscopy (ICP-AES) allowing estimating the weight percentage of S, V and Ce. These measurements were performed on a Horiba Jobin Yvon apparatus, Model Activa.

Specific surface area and pore volume measurements of the samples were done by N_2 physisorption at 77 K using a Micromeritics ASAP 2020 apparatus. The samples were outgassed in vacuum during 6 h at 200 °C prior the nitrogen physisorption.

X-ray diffraction patterns (XRD) were obtained using a MRD PRO PANalytical X'Pert PRO instrument with CuKα radiation (λ = 1.5418 Å) at the rate of 0.02°/s from 5 to 70 °C.

Total acidity was evaluated by temperature-programmed desorption of ammonia (TPD/NH_3) using a quadrupole Balzers QMC 311. Before NH_3 desorption, the samples were pre-treated under He flow (60 ml/min) at 200 °C for 1 h. NH_3 adsorption was performed under ambient conditions by flowing 0.5% NH_3 in He over the catalyst until saturation and then desorption of NH_3 by temperature-programmed treatment under He from 50 to 500 °C using a heating rate of 10 °C/min.

In situ diffuse reflectance infrared spectroscopy (DRIFTS) spectra were recorded on a Bruker IFS 55 spectrophotometer equipped with a Thermo Spectra Tech reacting cell at a spectral resolution of 4 cm^{-1} and accumulating 200 scans. Samples were treated in situ at 500 °C with helium (5 °C/min, flow: 30 cm^3/min).

Temperature programmed reduction (TPR) experiments were performed in a dynamic apparatus using 5% H_2 in helium flowing at 60 ml/min. Experiments were carried out in the range 30–800 °C. The inlet and outlet gas compositions were measured using a quadrupole mass spectrometer QMC 311 Balzers coupled to the reactor.

X-ray photoelectron spectra (XPS) were collected on a SSI X probe spectrometer (model SSI 100, Surface Science Laboratories, Mountain View, CA, USA) equipped with a monochromatized AlK_α radiation (1486 eV). The samples powders, pressed in small stainless steel troughs of 4 mm diameter, were placed on an insulating home made ceramic carousel. The pressure in the analysis chamber was around 10^{-6} Pa. The angle between the surface normal and the axis of the analyser lens was 55°. The analyzed area was approximately 1.4 mm^2 and the pass energy was set at 150 eV. The C1s peak of carbon has been fixed to 284.8 eV to set the binding energy scale. Data treatment was performed with the CasaXPS program (Casa Software Ltd., UK) and some spectra were decomposed with the least squares fitting routine provided by the software with a Gaussian/Lorentzian (85/15) product function and after subtraction of a non linear baseline.

Raman spectra were measured with a Dilor Instrument S.A. spectrometer with the 632 nm line of Ar ion laser as excitation source under ambient conditions. The number of scans is 10 and the time of accumulation is 10 s per scan.

2.3. Catalytic test

Catalytic tests were performed with 200 mg of catalyst (200–315 μm) diluted in 800 mg of inactive glass spheres with diameters in the range 315–500 μm in a metallic fixed-bed micro-reactor (PID Eng&Tech, Madrid, Spain) operating at atmospheric pressure and fully monitored by computer. The gas stream was composed of 100 ppm of chlorobenzene, 20 vol.% of O_2 and helium as diluting gas to obtain 200 ml/min (space velocity (VVH) = 37,000 h^{-1}). The reaction was run from 100 to 400 °C in a step mode with a 150 min plateau at each temperature investigated. Analysis of reactants and products was continuously performed by on line gas chromatography (GC).

3. Results and discussion

Theoretical and experimental chemical compositions of the investigated samples VTi, VTiS, VTiCe and VTiSCe are compared in Table 1. The results indicate that vanadium and cerium were successfully incorporated in the catalysts. For sulfated samples, differences between the theoretical and the experimental sulfur ratio could be attributed to the loss of some of the sulfur during calcinations [12].

The surface areas and pore diameters of Ti, TiS, TiCe and TiSCe supports (as references) and VTi, VTiS, VTiCe and VTiSCe catalysts, calcined at 500 °C are given in Table 2. All solids are classified as mesoporous materials (pores between 2 and 50 nm). It can be seen from this table that the specific surface area of TiO_2 support

Table 1
Element analysis and theoretical composition of VTi, VTiCe, VTiS and VTiSCe calcined at 500 °C.

Catalysts	Bulk composition (wt.%)			Theoretical composition (wt.%)		
	V	Ce	S	V	Ce	S
VTi	1.06			1.1		
VTiCe	1.08	14.22		1.1	14.4	
VTiS	1.09		2.2	1.1		8
VTiSCe	0.99	14.36	2.2	1.1	14.4	8

Table 2
Specific surface areas and mean pore size diameters of supports and catalysts calcined at 500 °C.

Sample	Surface area (m^2/g)	Pore diameter (Å)
Ti	115	80
TiCe	140	174
TiS	88	109
TiCeS	129	137
VTi	136	98
VTiCe	141	114
VTiS	114	82
VTiCeS	102	164

increases after incorporation of ceria. This observation indicates that the doping with CeO_2 is beneficial to the specific area of Ti material. Concerning the specific surface areas of unsulfated VTiCe and VTi, we note that they are quite similar. It indicates that the doping with CeO_2 allows preserving high specific surface area. The VTi catalyst was found to display greater surface area than the Ti support (136 m^2/g instead of 115 m^2/g). However, doping Ti or TiCe supports with sulfate groups induces a decrease in surface areas, which might be due to the collapse of some pores during the calcination [33]. Similarly, doping VTi and VTiCe samples with sulfate induces a decrease in surface areas. This contrasts with the case where VTiS catalysts were prepared in a one-step sol–gel procedure and in which the presence of sulfate had no impact on the texture [12]. Here the procedure is in two steps and the negative effect of sulfate observed in the present case takes place during the impregnation step.

Fig. 1 shows the XRD patterns of the vanadia-based catalysts and corresponding sulfated ones treated at 500 °C. No diffraction peaks due to crystalline vanadia oxide were detected, indicating that V_2O_5 species were (i) highly dispersed over TiO_2, TiO_2–SO_4^{2-}, TiO_2–CeO_2 and TiO_2–SO_4^{2-}–CeO_2 supports or (ii) having very small particle size. In addition, VTi and VTiS samples show only the diffraction

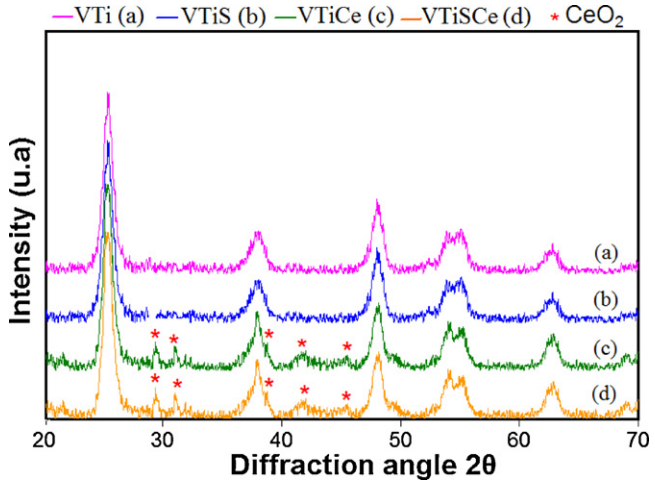

Fig. 1. X-ray powder diffraction patterns of VTi, VTiS, VTiCe and VTiSCe samples treated at 500 °C.

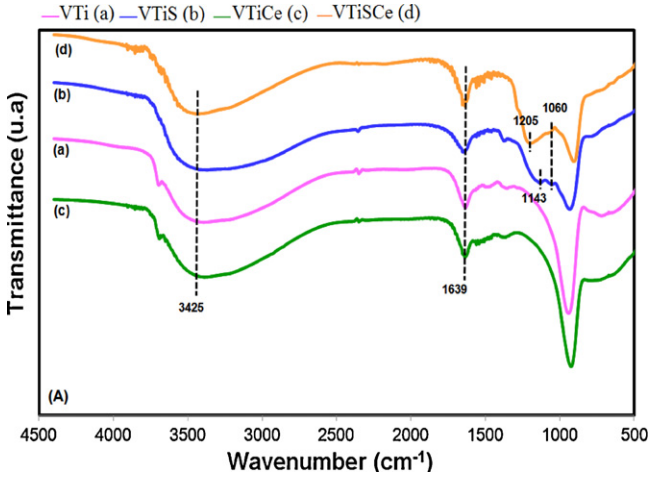

Fig. 2. DRIFTS spectra of VTi, VTIS, VTiCe and VTiSCe catalysts calcined at 500 °C.

peaks of the anatase phase with high crystallinity such as $2\theta = 25°$, 37°, 48° and 53° (PDF-ICDD 21-1272). However, solids doped with ceria exhibited both characteristic peaks of TiO_2 anatase and cubic CeO_2 phase (PDF-ICDD 34-0394).

The DRIFTS spectra of the prepared catalysts treated at 500 °C are given in Fig. 2. All solids exhibit bands at 3425 and 1639 cm^{-1} characteristic of stretching vibrations of O—H and bending vibrations of H—O—H, respectively. No bands related to vanadium species were detected in all samples, presumably because of the highly dispersed state of vanadium species in these samples and of the relatively V loading. For sulfated materials, bands at 1205, 1143 and 1060 cm^{-1} appeared and are assigned to vibration mode of sulfate species [34,35] confirming the involvement of sulfur in the catalytic structure.

Raman spectra of sulfated and unsulfated vanadia based catalysts are shown in Fig. 3. The set of peaks at 645, 520, 401 and 150 cm^{-1} belonging to anatase phase were observed for all the samples [36]. However, no typical Raman peaks around 995, 700, 525, 405, 301 and 282 cm^{-1} belonging to crystalline V_2O_5 were observed revealing the highly dispersed state of vanadium species in these samples [18]. Besides, the typical Raman signal of sulfate species (at 1370 cm^{-1}) [37] was not detected probably due to the low content of sulfate incorporated in our catalysts. These results are in accordance with the obtained XRD patterns. Moreover, Raman spectra did not show characteristic peak for CeO_2 around 458 cm^{-1} in catalysts doped with ceria [38,39]. This indicates the advantage to use

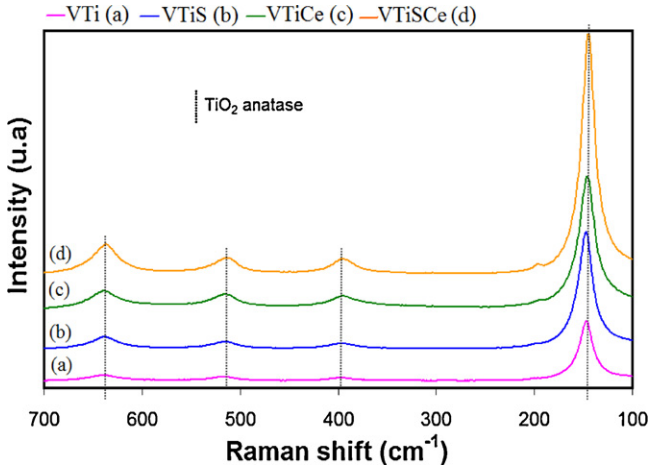

Fig. 3. Raman spectra of VTi, VTiS, VTiCe and VTiSCe samples treated at 500 °C.

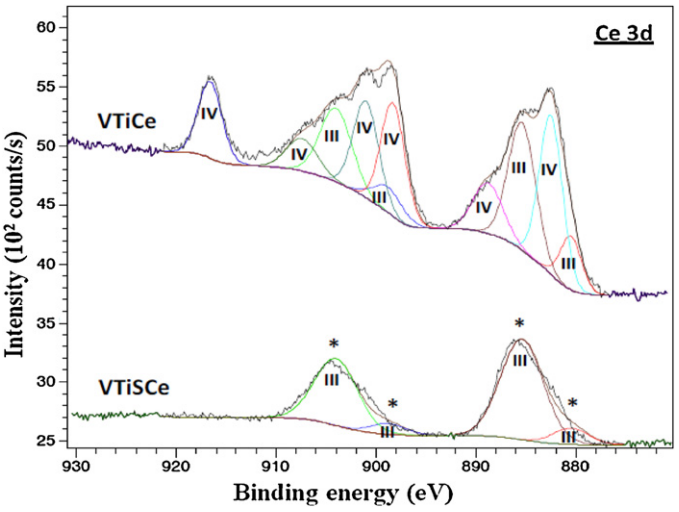

Fig. 4. Ce 3d XPS profile of VTi and VTiSCe catalysts calcined at 500.

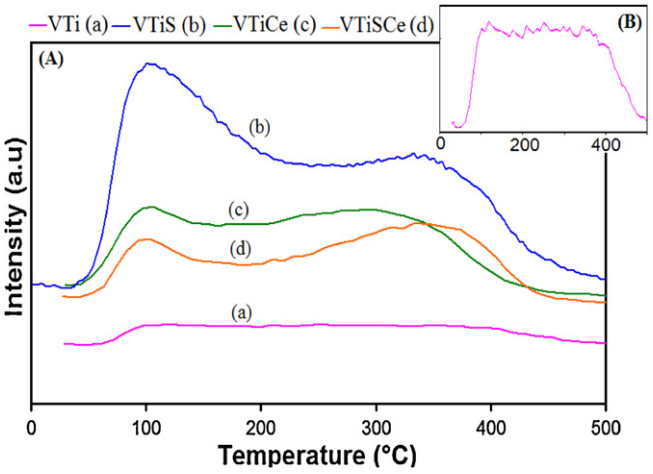

Fig. 5. NH_3-TPD profiles of VTi, VTiS, VTiCe and VTiSCe samples treated at 500 °C.

different techniques for the determination of surface structures of catalysts.

To investigate the surface composition of the catalysts, XPS measurements were performed. The binding energy values of the elements Ti 2p, S 2p and V 2p and the surface atomic ratios V/Ti, V/Ce, V/S and V/(Ce + S) are displayed in Table 3. The surface atomic ratio V/Ti increased in the presence of cerium species and decreased when sulfate groups are introduced in TiO_2 or TiO_2–CeO_2 supports revealing that vanadia spreads further on the surface of TiO_2 in the presence of cerium species and that Ce interacts with SO_4^{2-} groups. Similarly, sulfate groups decrease the spreading of vanadium species on CeO_2 since the surface atomic ratio V/Ce diminishes with sulfation. Besides, the decrease of V/S ratio after cerium incorporation in VTiS support is in favor of the interaction Ce–SO_4^{2-}.

The binding energies of Ti $2p_{3/2}$ for all catalysts were around 459 eV, characteristic of Ti^{4+} in TiO_2 [39,40]. This oxidation state remains unchanged for sulfated and unsulfated catalysts doped or not with ceria. A contribution with binding energies around 515 and 517 eV was detected for all samples containing vanadia, suggesting that vanadium, in this study, was present as a mixture of IV and V oxidation states [41,42]. The XPS binding energies of the O 1s spread over a wide range from 527 to 534 eV which could be assigned to the lattice oxygen associated with the metal oxides [43,44]. The interpretation is complicated due to the overlapping contributions of oxygen from titania, ceria, vanadia and from their mixed oxide compounds.

The Ce 3d XPS profiles of VTiCe and VTiSCe samples treated at 500 °C are shown in Fig. 4. V_2O_5/TiO_2–CeO_2 sample exhibits peaks due to the presence of both Ce^{4+} and Ce^{3+}, thus implying that cerium is present at the surface in both 4+ and 3+ oxidation states [43–45]. For VTiSCe catalyst, only Ce (III) is detected likely due to the interaction between cerium and sulfate species.

For sulfated catalysts, a peak with a binding energy near 169 eV was measured for the S 2p. According to literature, such an XPS band represents the existence of sulfate on the catalyst surface [37,46,47].

To evaluate the surface acidity of solid catalysts, NH_3-TPD experiments were carried out. The obtained profiles are shown in Fig. 5. The NH_3 desorption profile of the V_2O_5/TiO_2 sample shows two unresolved peaks at around 100 °C and 380 °C which could be attributed to NH_3 desorbed from weak and strong acidic sites, respectively [46–48] (Fig. 5(B)). The addition of sulfate groups to VTi or VTiCe samples enhances the total acidity of these catalysts proven by the increase of the intensities of the two peaks mentioned above. However, this effect is more remarkable for VTiS catalyst especially for the weak acidic peak (100 °C). These observations suggest that weak acid sites are more abundant on the surface of V_2O_5 supported on sulfated TiO_2 than on sulfated TiO_2 doped with ceria. Moreover, the enhancement of weak acidity is highly beneficial for the catalytic performances of V_2O_5/TiO_2 as discussed in earlier works [12,49–51]. Besides, it seems that cerium species create new acidic sites since VTiCe exhibits higher acidity than VTi, suggesting a progressive transformation of the surface acidity due to the cerium incorporation.

The reducibility of sulfate, vanadium and cerium species in the prepared catalysts was examined by means of H_2-TPR. Reference reduction curves of supports TiO_2 (Ti), TiO_2–SO_4^{2-} (TiS), TiO_2–CeO_2 (TiCe) and TiO_2–SO_4^{2-}–CeO_2 (TiSCe) are given in Fig. 6(A). The H_2-TPR profiles of the impregnated catalysts are shown in Fig. 6(B). For TiO_2 support, no H_2 peak consumption was observed. However, for the sulfated one, two peaks appeared at around 639 and 650 °C and are assigned to the reduction of sulfate species into SO_2 essentially as observed in earlier work [19,40]. After cerium incorporation, the TPR profile of the unsulfated support exhibits a weak peak centered at about 546 °C which could be attributed to a surface reduction of Ce^{4+} to Ce^{3+} [52,53]. Besides, it seems that the introduction of sulfate groups inhibits slightly the reduction of ceria since the cerium reduction peak at 548 °C shifted to higher temperatures (remarkable shoulder at 603 °C).

After vanadium impregnation, the TPR profile of the unsulfated catalyst prepared without cerium, exhibits a peak centered at about 491 °C which might be ascribed to the reduction of VO_x species [54,55]. Another peak centered at about 548 °C is observed after the cerium incorporation in this catalyst which is attributed to a surface reduction of CeO_2 as discussed below.

For VTiSCe sample, a reduction peak at around 680 °C with a shoulder at 657 °C is observed and can be assigned to the decomposition of sulfate species to essentially SO_2. It seems that the introduction of SO_4^{2-} succeeds to stabilize the vanadium and cerium at a higher oxidation state. In fact, the introduction of sulfate is observed to slightly inhibit the reduction of ceria and vanadia since the cerium reduction peak at 548 °C shifted to higher temperatures (shoulder at 587 °C) and the reduction of vanadium, occurring at that same temperature (587 °C) was completely hidden.

Moreover, when ceria is absent, the TPR position peak of sulfate in VTiS appears at lower temperature (567 °C) with shoulder at 546 °C. This result is in agreement with the fact that strong interactions between vanadium and sulfate species promote the

Table 3
XPS Binding energies and V/X (X = Ti, Ce and/or S) atomic ratios of the VTi, VTiCe, VTiS and VTiSCe impregnated catalysts calcined at 500 °C.

Catalyst	Binding energy (eV)				Atomic ratio V/X (X = Ti, Ce and/or S)			
	Ti $2p_{3/2}$	V $2p_{3/2}^{5+}$	V $2p_{3/2}^{4+}$	S 2p	V/Ti	V/Ce	V/S	V/(Ce + S)
VTi	458.6	517.2	515.9	–	0.032	–	–	–
VTiCe	458.5	517.3	515.7	–	0.077	0.778	–	–
VTiS	459.1	517.1	515.2	169.1	0.019		0.142	–
VTiSCe	459.0	517.1	515.9	169.0	0.042	0.469	0.132	0.1

sulfate reduction leading to better redox properties of vanadium supported on sulfated TiO_2.

Fig. 7 shows the evolution of the chlorobenzene conversion of the impregnated catalysts supported on TiO_2, TiO_2–SO_4^{2-}, TiO_2–CeO_2 and TiO_2–SO_4^{2-}–CeO_2 in the range 100–400 °C. Each temperature was maintained for 2h30 and stable levels of conversion were always observed. CO_2 is the main product. The carbon balance is completed with carbon monoxide, which is also produced especially at a relatively high temperature (from a few percent up to ca. 30%). No other partial oxidation products (chlorinated or not) are observed. These observations hold for all catalysts. It can be observed that the catalytic activity changes according to the nature of support. Vanadia impregnated on TiO_2–CeO_2 and TiO_2–SO_4^{2-}–CeO_2 present the best catalytic activity for the total oxidation of chlorobenzene and this activity is much higher than the corresponding catalyst without ceria (TiO_2 and TiO_2–SO_4^{2-}). There is a clear beneficial effect of the addition of ceria. In fact, the binary system VTi is virtually inactive for chlorobenzene conversion below 250 °C and exhibits a moderate activity above 300 °C (chlorobenzene conversion is only about 24% at this temperature (300 °C) and merely reaches 55% at 400 °C). The incorporation of ceria into this catalyst brings a marked improvement in catalytic activity also from 300 °C (chlorobenzene conversion increases to 71% at 300 °C and reaches total conversion at 400 °C). These observations pointed out the beneficial role of mixed oxide (CeO_2–TiO_2) support compared to the corresponding single oxide (TiO_2) in the enhancement of the catalytic activity of vanadia based catalysts in chlorobenzene oxidation at high temperature. This improvement of the activity can be attributed to the redox properties of cerium existing in CeO_2 form in all the prepared catalysts as shown by XRD technique. This result is consistent with that of literature [28,56]. In fact, CeO_2 has the ability to adsorb, store and transfer surface oxygen species and presumable supplies active oxygen to the vanadium species that are reduced during the catalytic reaction.On the other hand, the sulfation of catalysts doped or not with ceria, brings an increase of catalytic activities especially in the range 200–300 °C since VTiS and VTiSCe begin to convert, respectively, 23 and 15% of chlorobenzene at 200 °C, convert 62% and 83% at 300 °C, and both reach total conversion at 400 °C. These observations highlight the importance of sulfate groups on the catalytic activity at lower temperatures. In fact, sulfates on the surface of vanadia based catalysts significantly affect both the redox and the acidic properties of these materials as shown by H_2-TPR and NH_3-TPD experiments. This result corroborates with previous researches which showed that the interaction between sulfate groups and vanadium species enhances the reducibility of VTiS material and the reactivity of vanadium redox sites, leading to more active catalysts [20,51,53]. Nonetheless, we note that the beneficial effect of sulfation is further enhanced when the catalyst is prepared in the presence of cerium species. This observation could be attributed to the strong interaction between ceria and sulfates at the surface as evidenced by TPR and XPS studies and discussed above. This interaction increases the redox properties of VTiSCe catalyst. This

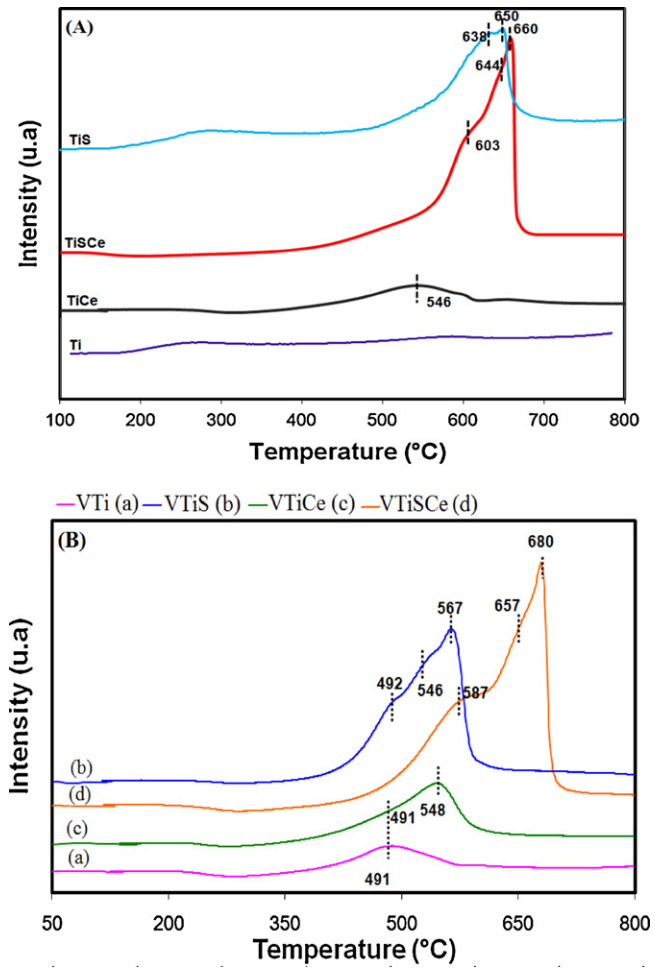

Fig. 6. H_2-TPR profiles of the samples treated at 500 °C, (A) H_2-TPR profiles of Ti, TiS, TiCe and TiSCe supports, (B) H_2-TPR profiles of VTi, VTiS, VTiCe and VTiSCe impregnated catalysts.

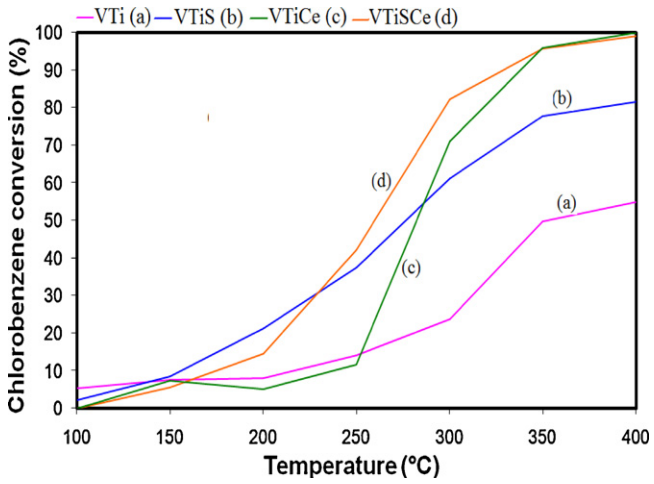

Fig. 7. Chlorobenzene conversion over vanadia supported catalysts.

improvement of redox properties leads to the increased reactivity of VTiCe for chlorobenzene conversion compared to the ternary VTiS sample.

4. Conclusion

In the present investigation, a series of TiO_2, TiO_2–SO_4^{2-}, TiO_2–CeO_2 and TiO_2–SO_4^{2-}–CeO_2 aerogel supports is prepared by a sol gel route and active vanadia is deposited by impregnation method. Catalytic tests indicate that Ce-doped V_2O_5-based catalysts achieve 100% chlorobenzene conversion at 400 °C. This could be related to the redox properties of cerium existing in the form of CeO_2 in the prepared catalysts. Besides, sulfate containing vanadia–titania samples prepared with or without ceria had considerably improved catalytic properties in the chlorobenzene oxidation in the lower temperature range (200–300 °C) as compared to corresponding unsulfated catalysts. In fact, sulfation generates additional weak acidic sites at the catalyst surface. This likely promotes the chlorobenzene adsorption. As sulfation also improves the redox properties of both vanadium and cerium species at the surface of catalysts, a marked increase in activity is observed. This is due to the existence of strong interaction between vanadia and sulfate on the one hand, and between ceria and sulfate on the other hand. This superficial interaction induces a higher reactivity of redox sites leading to higher efficiency of catalysts.

References

[1] C. Gennequin, M. Lamallem, R. Cousin, S. Siffert, V. Idakiev, T. Tabakova, A. Aboukaìs, B.L. Su, J. Mater. Sci. 44 (2009) 6654–6662.
[2] Z. Minghui, L. Pengyan, B. Zhicheng, X. Xiaobai, Chin. Sci. Bull. 44 (1999) 1249–1257.
[3] A. Buekens, H. Huang, J. Hazard. Mater. 62 (1998) 1–33.
[4] J.D. Kilgroe, J. Hazard. Mater. 47 (1996) 163–194.
[5] R. Weber, M. Plinke, Z.T. Xu, M. Wilken, Appl. Catal. B: Environ. 31 (2001) 195–207.
[6] A. Andersson, C. Rappe, O. Maaskant, J. Unsworth, S. Marklund, Organohalogen. Compd. 36 (1998) 109–112.
[7] S. Andersson, S. Kreisz, H. Hunsinger, Filtr. Sep. 40 (2003) 22–25.
[8] Y. Liu, Z. Wei, Z. Feng, M. Luo, P. Ying, C. Li, J. Catal. 202 (2001) 200–204.
[9] K. Everaert, J. Baeyens, J. Hazard. Mater. 109 (2004) 113–139.
[10] R. Delaigle, D.P. Debecker, F. Bertinchamps, E.M. Gaigneaux, Top. Catal. 52 (2009) 501–516.
[11] D.P. Debecker, R. Delaigle, P.C. Hung, A. Buekens, E.M. Gaigneaux, M.B. Chang, Chemosphere 82 (2011) 1337–1342.
[12] C. Gannoun, R. Delaigle, P. Eloy, D.P. Debecker, A. Ghorbel, E.M. Gaigneaux, Catal. Commun. 15 (2011) 1–5.
[13] J. Lichtenberger, M.D. Amiridis, J. Catal. 223 (2004) 296–308.
[14] S. Lomnicki, J. Lichtenberger, Z. Xu, M. Waters, J. Kosman, M.D. Amiridis, Appl. Catal. B: Environ. 46 (2003) 105–119.
[15] L. Owens, H.H. Kung, J. Catal. 144 (1993) 202–213.
[16] F. Arena, F. Frusteri, A. Parmaliana, Appl. Catal. A: Gen. 176 (1999) 189–199.
[17] F. Bertinchamps, C. Gregoire, E.M. Gaigneaux, Appl. Catal. B: Environ. 66 (2006) 1–9.
[18] Q. Sun, Y. Fu, J. Liu, A. Auroux, J. Shen, Appl. Catal. A: Gen. 334 (2008) 26–34.
[19] L. Baraket, A. Ghorbel, P. Grange, Appl. Catal. B: Environ. 72 (2007) 37–43.
[20] S.T. Choo, Y.G. Lee, I.S. Nam, S.W. Ham, J.B. Lee, Appl. Catal. A: Gen. 200 (2000) 177–188.
[21] H. Zhao, S. Bennici, J. Shen, A. Auroux, J. Mol. Catal. A 309 (2009) 28–34.
[22] B. Murugan, A.V. Ramaswamy, J. Am. Chem. Soc. 129 (2007) 3062–3063.
[23] C.T. Campbell, C.H.F. Peden, Science 309 (2005) 713–714.
[24] J. Rynkowski, J. Farbotko, R. Touroude, L. Hilaire, Appl. Catal. A: Gen. 203 (2000) 335–348.
[25] S.X. Yang, W.P. Zhu, Z.P. Jiang, Z.X. Chen, J.B. Wang, Appl. Surf. Sci. 252 (2006) 8499–8505.
[26] M.F. Luo, J. Chen, L.S. Chen, J.Q. Lu, Z.C. Feng, C. Li, Chem. Mater. 13 (2001) 197–202.
[27] K. Josef Antony Raj, B. Viswanathan, Indian J. Chem. A 49 (2010) 401–406.
[28] Y. Huang, Z. Tong, B. Wu, J. Zhang, J. Fuel Chem. Technol. 36 (2008) 616–620.
[29] W.Q. Xu, Y.B. Yu, C.B. Zhang, H. He, Catal. Commun. 9 (2008) 1453–1457.
[30] X. Gao, Y. Jiang, Y. Fu, Y. Zhong, Z. Luo, K. Cen, Catal. Commun. 11 (2010) 465–469.
[31] W. Shan, F. Liu, H. He, X. Shi, C. Zhang, Catal. Today 184 (2012) 160–165.
[32] L.J. Alemany, F. Berti, G. Busca, G. Ramis, D. Robba, G.P. Toledo, M. Trombetta, Appl. Catal. B: Environ. 10 (1996) 299–311.
[33] H. Zhao, S. Bennici, J. Cai, J. Shen, A. Auroux, J. Catal. 274 (2010) 259–272.
[34] C. Morterra, G. Cerrato, M. Signoretto, Catal. Lett. 41 (1996) 101–109.
[35] M. Bensitel, O. Saur, J.C. Lavalley, B.A. Morrow, Mater. Chem. Phys. 19 (1988) 147–156.
[36] B.M. Reddy, A. Khan, Y. Yamada, T. Kobayashi, S. Loridant, J.C. Volta, J. Phys. Chem. B 107 (2003) 5162–5167.
[37] J.P. Chen, R.T. Yang, J. Catal. 139 (1993) 277–288.
[38] J. Matta, D. Courcot, E. Abi-Aad, A. Aboukaìs, Chem. Mater. 14 (2002) 4118–4125.
[39] P. Fornasiero, G. Balducci, R. Di Monte, J. Kâspar, V. Sergo, G. Gubitosa, A. Ferrero, M. Graziani, J. Catal. 164 (1996) 173–183.
[40] J.P. Nogier, M. Delamar, Catal. Today 20 (1994) 109–123.
[41] V.I. Bukhtiyarov, Catal. Today 56 (2000) 403–414.
[42] G. Silversmit, D. Depla, H. Poelman, G.B. Marin, R. De Gryse, J. Electron. Spectrosc. Relat. Phenom. 135 (2004) 167–175.
[43] B.M. Reddy, K.N. Rao, G.K. Reddy, A. Khan, S.-E. Park, J. Phys. Chem. C 111 (2007) 18751–18758.
[44] B.M. Reddy, P. Bharali, P. Saikia, A. Khan, S. Loridant, M. Muhler, W. Grunert, J. Phys. Chem. C 111 (2007) 10478–10483.
[45] B.M. Reddy, K.N. Rao, G.K. Reddy, P. Bharali, J. Mol. Catal. A: Chem. 253 (2006) 44–51.
[46] S.T. Choo, Y.G. Lee, I.-S. Nam, S.W. Ham, J.B. Lee, Appl. Catal. A: Gen. 200 (2000) 177–188.
[47] M.H. Kim, L.-S. Nam, Y.G. Kim, J. Catal. 179 (1998) 350–360.
[48] L. Chmielarz, P. Kustrowski, M. Zbroja, W. Lasocha, R. Dziembaj, Catal. Today 90 (2004) 43–49.
[49] F. Bertinchamps, C. Grégoire, E.M. Gaigneaux, Appl. Catal. B: Environ. 66 (2006) 10–22.
[50] J. Arfaoui, L. Khalfallah Boudali, A. Ghorbel, Appl. Clay Sci. 48 (2010) 171–178.
[51] D.P. Debecker, F. Bertinchamps, N. Blangenois, P. Eloy, E.M. Gaigneaux, Appl. Catal. B: Environ. 74 (2007) 223–232.
[52] H.C. Yao, Y.F. Yu Yao, J. Catal. 86 (1984) 254–265.
[53] X. Gu, J. Ge, H. Zhang, A. Auroux, J. Shen, Thermochim. Acta 451 (2006) 84–93.
[54] H. Poelman, B.F. Sels, M. Olea, K. Eufinger, J.S. Paul, B. Moens, I. Sack, V. Balcaen, F. Bertinchamps, E.M. Gaigneaux, P.A. Jacobs, G.B. Marin, D. Poelman, R. De Gryse, J. Catal. 245 (2007) 156–172.
[55] G.Y. Popova, T.V. Andrushkevich, E.V. Semionova, Y.A. Chesalov, L.S. Dovlitova, V.A. Rogov, V.N. Parmon, J. Mol. Catal. A: Chem. 283 (2008) 146–152.
[56] E. Tronconi, I. Nova, C. Ciardelli, D. Chatterjee, M. Weibel, J. Catal. 245 (2007) 1–10.